

Strontium Aluminate/Polymer Composites: Morphology, Luminescent Properties, and Durability

S. B. Mishra,^{1,2} A. K. Mishra,^{1,2} N. Revaprasadu,³ K. T. Hillie,⁴ W. J. vdM. Steyn,^{2,5}
E. Coetsee,¹ H. C. Swart¹

¹Department of Physics, University of the Free State, Bloemfontein, ZA9300, Republic of South Africa

²CSIR Built Environment, CSIR, Pretoria, ZA 0001, Republic of South Africa

³Department of Chemistry, University of Zululand, Kwadlangezwa 3886, Republic of South Africa

⁴National Centre for Nano-Structured Materials, CSIR, Pretoria, ZA 0001, Republic of South Africa

⁵Department of Civil Engineering, University of Pretoria, ZA 0001, Republic of South Africa

Received 11 April 2008; accepted 25 October 2008

DOI 10.1002/app.29933

Published online 6 March 2009 in Wiley InterScience (www.interscience.wiley.com).

ABSTRACT: Phosphor-based polymer composites were prepared using a melt mixing and extrusion method. Morphology, luminescent properties, and Hamburg wheel test (HWT) of synthesized hybrid material were studied using various polymer matrices. The intensities of the luminescence of the strontium aluminates phosphors ($\text{SrAl}_2\text{O}_4 : \text{Eu,Dy}$ and $\text{Sr}_4\text{Al}_{14}\text{O}_{25} : \text{Eu,Dy}$) were substantially changed when incorporated into structurally and chemically different organic matrices. HWTs were performed to evaluate the durability of the polymers against simulated wheel loads and the effect of

these wheel loads on the luminosity of the polymers. The decay slopes of various polymer-phosphor composites suggests that the simulated wheel load of the Hamburg test did not have a profound effect on the luminosity as such but the duration of luminescence was found to be shorter for the polymer-phosphor hybrid after the Hamburg test. © 2009 Wiley Periodicals, Inc. *J Appl Polym Sci* 112: 3347–3354, 2009

Key words: strontium aluminate; composite; morphology; photoluminescence; decay slopes; Hamburg wheel test

INTRODUCTION

The unique optical and electrical properties of semiconductor matter have opened up new areas of research and development.¹ Europium (Eu^{2+})-doped strontium aluminate phosphors have long afterglow properties and have high quantum efficiency.^{2,3} Strontium aluminate doped with Eu show blue-green luminescence due to the $5d \leftrightarrow 4f$ transition in the Eu^{2+} ions. The phosphorescence phenomenon can be prolonged by codoping of this phosphor with rare earth ions such as Dy or Nd ions or inclusions of tens of mol percent more of Al_2O_3 than the stoichiometry.^{4,5} Because of these properties, these phosphors have a wide variety of applications, including luminous paints in highways, airports, buildings, ceramic products, textiles, outdoor nighttime displays, luminous clocks, and safety warnings.^{6–11} It can also be used for glow watches, textile escape routines, instruments, and warning signs. Besides, these phosphors are known to be chemically stable, safe, have

excellent photo resistance, are bright, and have long-lasting photoluminescence (PL).^{12–14}

Tailoring properties of multifunctional advanced materials through the combination of organic and inorganic components forming a composite material are gaining attention for various applications.¹⁵ The inorganic and organic phases linked together by weak interactions such as hydrogen, van der Waals, or ionic bonds is known as “Class-I hybrid” or physical hybrid. If these two phases are covalently bonded, the biphasic material is known as “Class-II hybrid” or chemical hybrid.¹⁶ Incorporating luminescent materials into polymer matrices allow these materials to be thermally and mechanically stable with good transparency, impact resistance, low temperature processibility leading to some potential applications in catalysis, sorption, optical devices, and magnetism.^{17–19} Recently, many scientists across the world have developed various methods for dispersing the phosphor into the polymer matrices. Wang et al.¹ prepared $\text{ZnS} : \text{Cu/PVA}$ composite nanofiber via electrospinning through coordination between $-\text{OH}$ and $\text{Zn}^{2+} : \text{Cu}$, which prevented the phosphor nanoparticles from aggregation in nanofibers. In another study, composite resin-containing lanthanide complexes were prepared by bulk-free radical copolymerization of lanthanide complexes, α -methylacrylic acid, and styrene, which show sharper

Correspondence to: H. C. Swart (swarthc.sci@ufs.ac.za).

Contract grant sponsors: National Research Foundation (NRF) of South Africa, Council for Scientific and Industrial Research (CSIR) of South Africa.

emission lines and higher intensities in composite resins.²⁰ Physical hybrids of Eu³⁺-doped siloxane-polyethylene glycol were prepared using sol-gel technique with an improved mechanical strength and glass transition temperature.¹⁵ Polymethacrylate/rare earth composite luminescent materials were formed through grafting via emulsion polymerization of methylmethacrylate onto the surface of luminescent materials that show better luminosity and water resistance.²¹ Gadolinium-doped Yttrium oxide that emits ultraviolet luminescence was synthesized by simple heating of precursor in a polymer solution. This material can be used as a ultraviolet (UV) source for activating titanium dioxide nanocatalysts on decomposing pollutants in water and air.²² Surface-initiated atom transfer radical polymerization was used to fabricate luminescent nanoparticle/polymer composite film.²³ Polymer/Cu₂S nanoparticles films were fabricated via layer-by-layer assembly method.²⁴

Melt mixing followed by extrusion or melt press is a popular technique to disperse fillers into the polymer matrix in the molten state. The technique allows all kinds of polymer to form composites and nanocomposites, which otherwise are difficult to process by other techniques for developing composite materials. Further, this technique does not require any solvent and thus becomes an environmentally sound and economically feasible.²⁵ So far, no reports have been found for fabricating polymer-phosphor composite using melt mixing and extrusion. The objective of this work is to disperse strontium aluminate phosphors into various polymer matrices, which differ in their structural and physical behaviors such as resistance to UV and opacity. The Hamburg test (a standard road pavement test) was used to evaluate the effect on the luminosity and the durability of the polymer-phosphor composite to simulated traffic load. The morphology and PL properties of the prepared composites were also studied.

EXPERIMENTAL

Materials

Low-density polyethylene (LDPE) (MFI 7 g/10 min), linear low-density polyethylene (LLDPE) (MFI 1 g/10 min), high-density polyethylene (HDPE), and polypropylene (PP) (MFI 12 g/10 min) were supplied by Sasol Polymers (Vanderbijlpark, South Africa). PP-grafted malice anhydride [(PP-g-MA-OPTIM-415), reactive modifier, MAH content = 1 wt %; density 0.91 g/cm³; melting point error = 160°C] was supplied by Pluss Polymers, India. Commercially available SrAl₂O₄ : Eu,Dy and Sr₄Al₁₄O₂₅ : Eu,Dy were obtained from Phosphor Technology (UK). The density and the melting point of these polymers are given in Table I.

TABLE I
Physical Property of the Various Polymers

Polymer	Density (g/cm ³)	Melting point (°C)	UV resistance	Opacity
LDPE	0.918	106	Poor	Translucent
LLDPE	0.924	124	Good	Translucent
HDPE	0.95	130	Poor	Opaque
PP	0.9	160	Poor	Translucent
PP-g-MA	0.91	160	Poor	Opaque

Preparation of nanocomposites

Polymers and phosphors were dried in an oven at 90°C overnight. These were melt blended using a Brabender mixer followed by extrusion. 3% by weight of the phosphors was mixed with various polymers for 30 min at 10°C higher than the melting point of polymer at a screw speed of 60 rpm. The samples were then extruded at an extrusion speed of 60 rpm at 130°C to obtain films with an average thickness of 0.45 ± 0.05 mm and an average width of 15 ± 1 mm.

SEM, SEM-EDX, and TEM

Scanning electron microscope (SEM) analyses of the nanocomposites were performed using a JEOL WIN-SEM-6400 electron microscope. The probe size was 115 nm, the probe current was 0.02 nA, the noise reduction was 64 Fr, and the AC voltage was 5.0 keV. The surfaces of the samples were coated with gold by an electrode deposition method to impart electrical conductivity before recording the SEM micrographs.

The SEM-EDX analyses were done in a Shimadzu SSX-550 SEM at an AC voltage of 15.00 kV and a working distance of 17 mm.

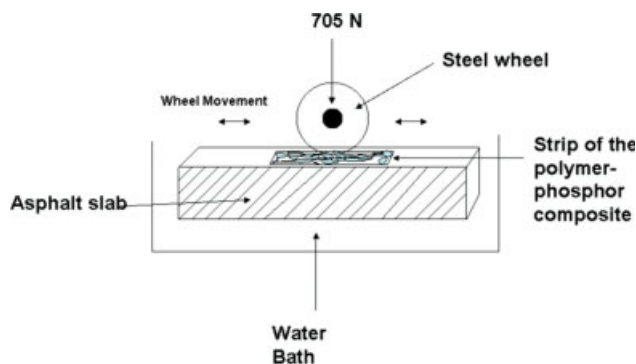
The transmission electron microscope (TEM) samples were prepared using cryoultramicrotomy. They were mounted on cryopins and frozen in liquid nitrogen. Sections were cut at -100°C using a Reichert FCS (Leica, Vienna, Austria) attached to a Reichert Ultracut S Ultramicrotome. The sections (100–150 nm thick) were collected on copper grids and viewed in a LEO 912 Omega (Carl Zeiss NTS GmbH, Oberkochen, Germany) TEM, with an energy filter operating at 120 kV.

Photoluminescence

PL was measured using a Varian Cary Eclips Fluorescence spectrophotometer with a Xe flash lamp. The samples were excited at a wavelength of 320 nm.

Hamburg wheel test

The Hamburg wheel test (HWT) consists of a water bath in which asphalt slabs are embedded while



Scheme 1 Schematic diagram of Hamburg Wheel Test.

being traversed with a smooth test wheel exerting a load of 705 N onto the samples. In this application, composite samples of length of 5 cm, width of 1 cm, and thickness of 0.5 mm were attached to the surface of the asphalt slab while the slab was exposed to the action of the test wheel. The procedure is shown in Scheme 1. This was done to measure the durability of the composite samples placed on the asphalt slabs against simulated traffic loads. The luminescence of the samples was measured using light-dependent resistor before and after applying various loading regimes.

RESULTS AND DISCUSSION

Morphological studies

The SEM images of pure $\text{SrAl}_2\text{O}_4 : \text{Eu,Dy}$ and $\text{Sr}_4\text{Al}_{14}\text{O}_{25} : \text{Eu,Dy}$ phosphors are shown in Figure 1(a,b). The images show irregular agglomerates in the range of 8–80 μm . Barring HDPE, the SEM micrographs of pristine LDPE [Fig. 1(c)], LLDPE, PP, and PP-g-MA demonstrate a hollow leaflet pattern. The formation of the leaflet pattern is probably due to the shear force of the extruder on which melted pristine polymers and polymer/phosphor composites fell to form the thin strips. Interestingly, LDPE, PP, and PP-g-MA-based phosphor composites show the tubular leaf pattern; however, randomly oriented bright lines [Fig. 1(d)] were observed from the SEM image of the LLDPE-phosphor composite. These types of different leaf patterns and other morphologies observed for various polymer-phosphor composites prepared under similar experimental conditions suggest that the physical properties like density and viscosity of the polymers would be the probable factors behind the different surface morphologies. In the case of LDPE- and PP-based phosphor composites [Figs. 1(e,f)], well-defined bridged leaflets are visible, whereas PP-g-MA-phosphor composite [Fig. 1(g)] shows an unbridged leaf pattern. Dispersed phosphor particles and some large agglomerates in the matrix were also observed on the high-magnifi-

cation images. The SEM micrographs of pure HDPE and HDPE-phosphor composites [Fig. 1(h)] with the highest density of the matrix, however, did not show any pattern.

The SEM-EDX mappings of the $\text{LDPE-Sr}_4\text{Al}_{14}\text{O}_{25} : \text{Eu,Dy}$ composite are shown in Figure 1(i). Carbon (C), oxygen (O), strontium (Sr), and aluminum (Al) elements in the composite were detected from SEM-EDX mappings. Because of the low concentration of the doped rare earth elements, SEM-EDX could not detect any Eu or Dy. The mappings of the $\text{LDPE-Sr}_4\text{Al}_{14}\text{O}_{25} : \text{Eu,Dy}$ composite show that the elements C, O, and Sr are evenly distributed in the leaflet pattern. The Al concentration was not high enough to clearly distinguish the leaflet structure on the Al. C is the major component of the LDPE, whereas Al belongs to the strontium aluminate used as filler. The O is present in the LDPE copolymer and the aluminates. The SEM-EDX mapping of the rest of the samples were quite similar to Figure 1(i).

A TEM image of the $\text{LDPE-Sr}_4\text{Al}_{14}\text{O}_{25} : \text{Eu,Dy}$ composite is shown in Figure 1(j). The leaflet structure again is visible. Unfortunately, the 100- to 150-nm-thick sections were still too thick to clearly see the phosphor material. Inset A, however, is an image of a slightly damaged part of the composite. The black spots on the edges clearly show the particle distribution of the phosphor material inside the polymer. The melt processing and extrusion allow the phosphor particles to uniformly disperse in the polymer matrix. No large agglomerates of phosphor particles were observed in the TEM micrographs. From TEM micrographs, not all shown here, it can be deduced that good compatibility exists between the polymer matrix and the phosphors.

Photoluminescence

Table I shows the optical behavior and resistance of various polymers toward UV light. Excitation of phosphors with UV light (320 nm) produced emission spectra at $\lambda = 520 \text{ nm}$ for $\text{SrAl}_2\text{O}_4 : \text{Eu,Dy}$ showing bright green luminescence and at $\lambda = 495 \text{ nm}$ for $\text{Sr}_4\text{Al}_{14}\text{O}_{25} : \text{Eu,Dy}$ with the blue luminescence, respectively. The emissions of pure phosphors and polymer-phosphor composites show a single peak with only one band.¹⁴ The crystal field at the sites of the luminescent ions and the degree of covalence (coordination number) of these ions with the surrounding O atoms are the two fundamental aspects that are responsible for the emission of the phosphor.^{26,27} The crystal field allows splitting of the 5d level into sublevels, which show that luminescence bands of phosphor are quite sensitive to the refractive index of the polymer matrix. There is a linear relationship between wavelength corresponding to

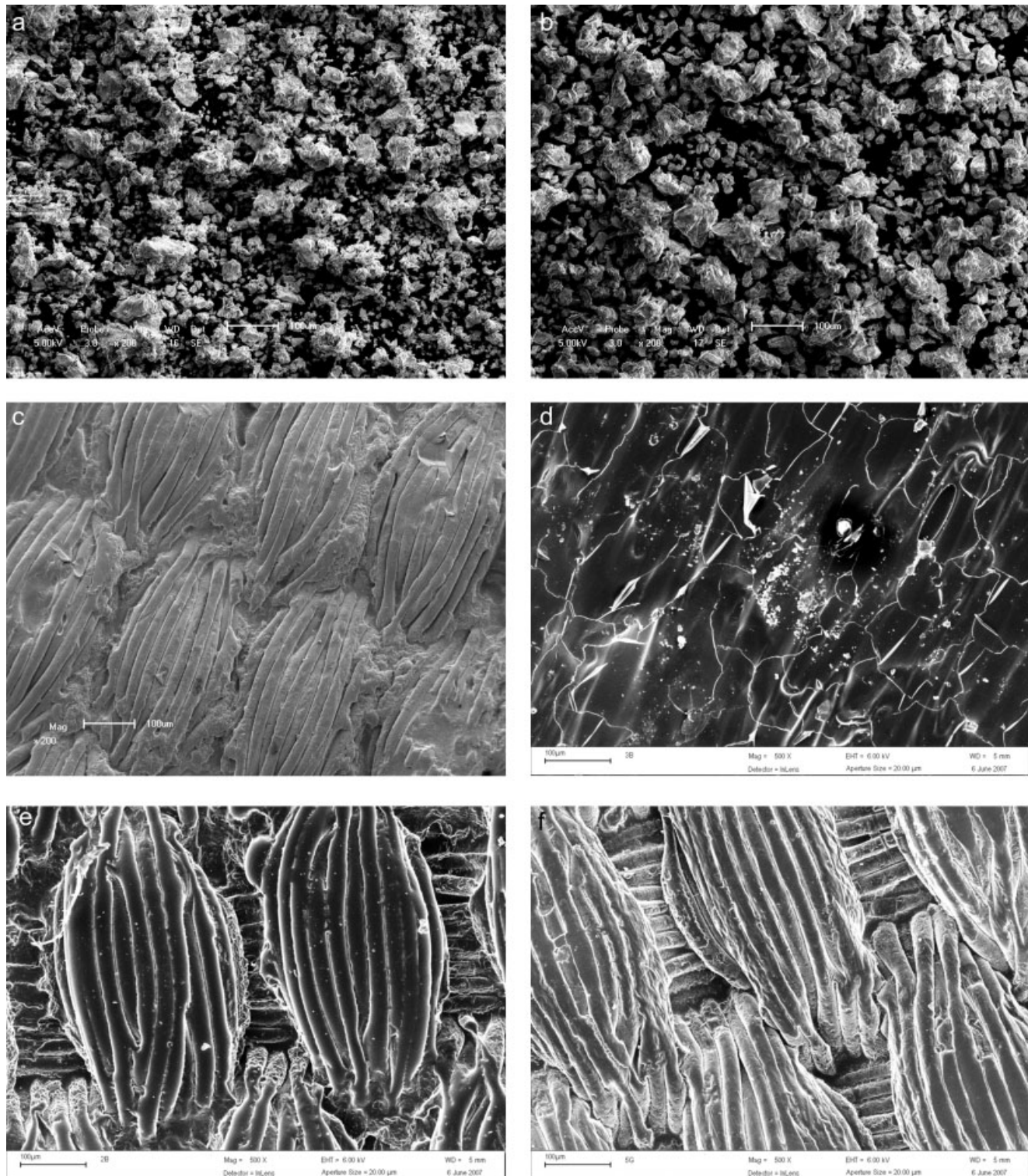


Figure 1 a: SEM image of the SrAl₂O₄:Eu,Dy phosphor powder; b: SEM image of the Sr₄Al₁₄O₂₅:Eu,Dy phosphor powder; c: SEM image of pure LDPE; d: SEM image of LLDPE-phosphor composite; e: SEM image of LDPE-phosphor composite; f: SEM image of PP-phosphor composite; g: SEM image of PP-g-MA-phosphor composite; h: SEM image of pure HDPE; i: SEM-EDS of Polymer-Phosphor composite; j: TEM image of LDPE phosphor composite. Inset A from damage part to show distribution of phosphor inside the polymer. [Color figure can be viewed in the online issue, which is available at www.interscience.wiley.com.]

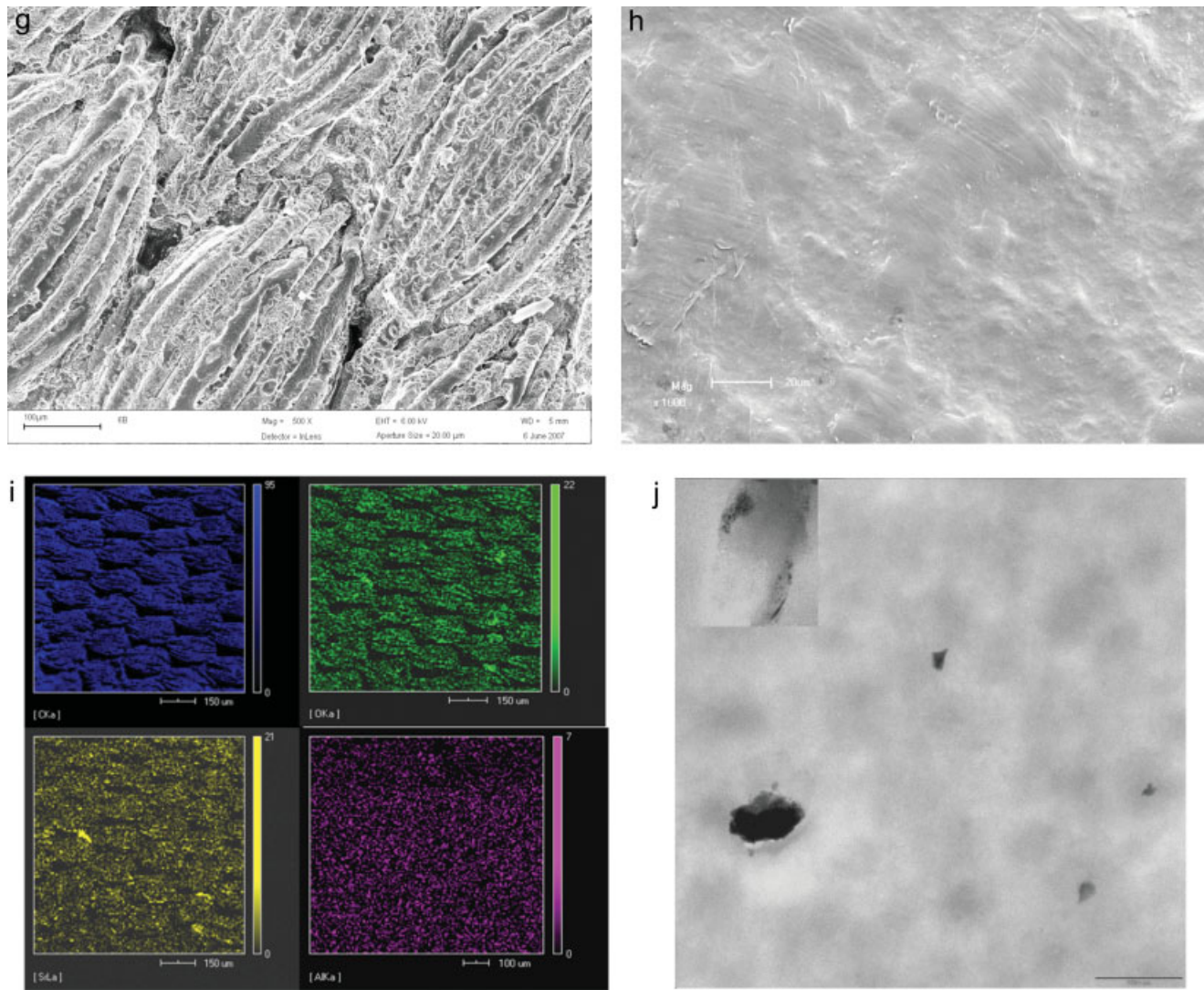


Figure 1 (Continued from the previous page)

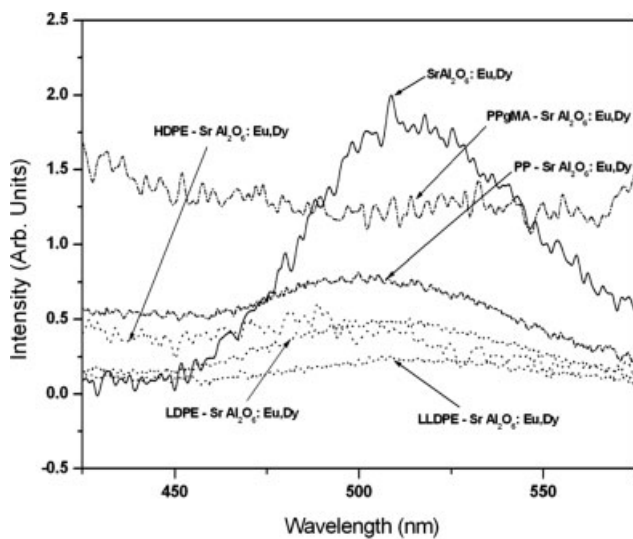


Figure 2 Photoluminescence spectra of SrAl₂O₄:Eu,Dy and Polymer-SrAl₂O₄:Eu,Dy composites.

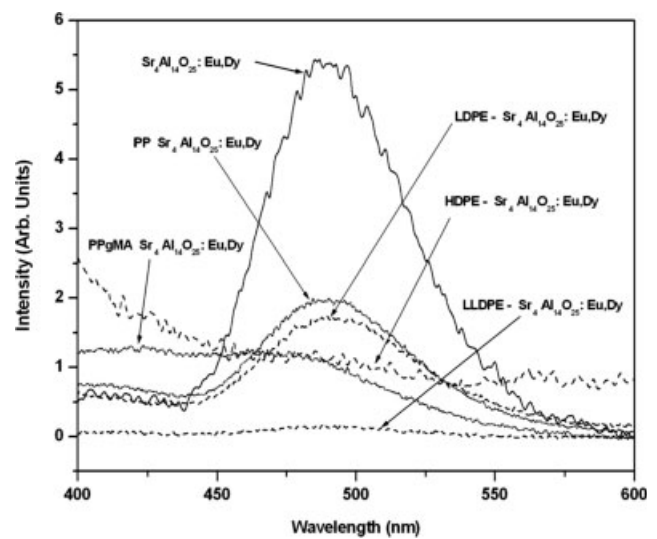
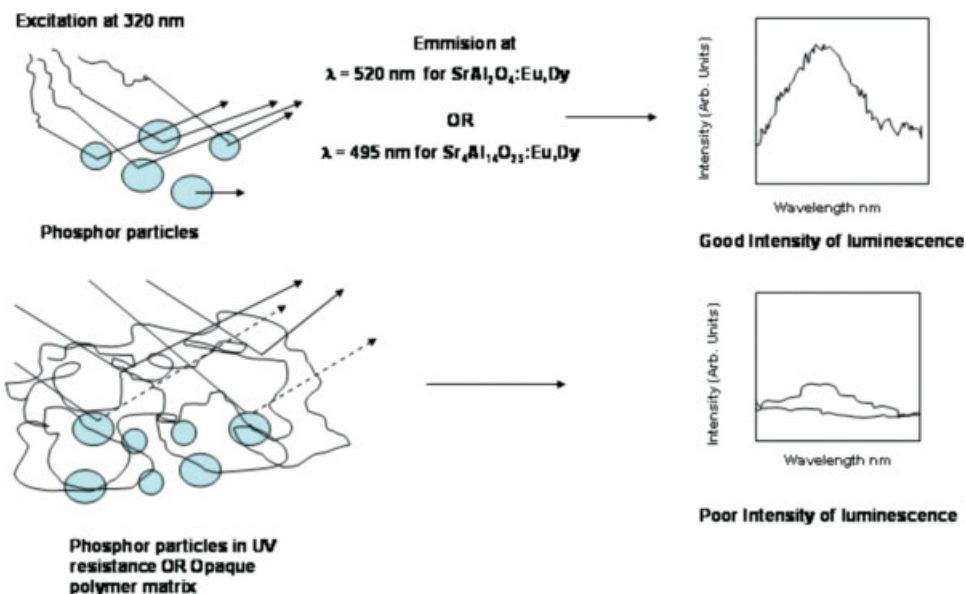


Figure 3 Photoluminescence spectra of Sr₄Al₁₄O₂₅:Eu,Dy and Polymer-Sr₄Al₁₄O₂₅:Eu,Dy composites.



Scheme 2 A schematic description of the excitation of the phosphor and polymer-phosphor composites.

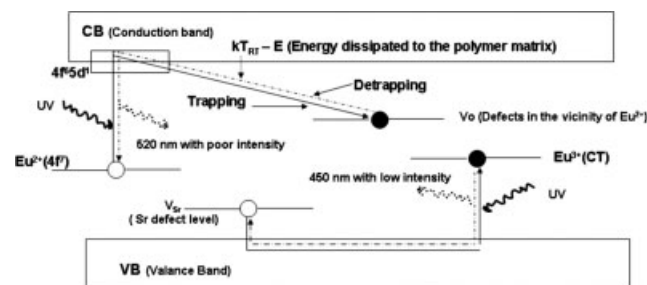
emission maximum and refractive index term, $n^2 - 1/2n^2 + 1$.²⁸

The emission spectra of pure $\text{SrAl}_2\text{O}_4 : \text{Eu,Dy}$ shows an intensity of 2 (Arbitrary units), whereas the intensity of $\text{Sr}_4\text{Al}_{14}\text{O}_{25} : \text{Eu,Dy}$ was found to be 5.5 (Arbitrary units), Figures 2 and 3. Because the melt mixing and extrusion was carried out at the temperature 10°C higher than the melting point of respective polymers, we expect no structural disturbance in the crystal structure of the phosphor. Further, the phosphorescent properties of strontium aluminate get affected only at 1090°C . The luminescence intensities of the polymer-phosphor composites were found to be lower than that of the pure phosphors. One of the probable reasons could be attributed to the fact of transparency and resistance of the polymer matrices for UV radiations. The amount of phosphors present in the composite material would also be a reason for the lower luminosity. Among the various polymers that were used for making luminescent composite material, LLDPE is known to have the best resistance for UV light and thus the matrix would not allow enough radiation to penetrate through the bulk to excite the phosphors. This may be attributed to the probable reason behind the poor emission of LLDPE- $\text{SrAl}_2\text{O}_4 : \text{Eu,Dy}$ and LLDPE- $\text{Sr}_4\text{Al}_{14}\text{O}_{25} : \text{Eu,Dy}$ composites as shown in Figures 2 and 3, respectively. A schematic description of the excitation process of the phosphor and the polymer-phosphor composites is shown in Scheme 2.

The opacity of the polymers toward UV radiations also effectively influences the luminescent intensity of polymer-phosphor composites as shown in Figures 2 and 3. The intensity of the emission peak for the polymer-phosphor composites decreases when

compared with the pure phosphors. This may be due to the presence of polymers in which the opacity and UV resistance (Table I) differ from each other in the polymer-phosphor composites.

Based on the experimental evidences, the mechanism for the 520 nm ($4f^65d^1-4f^7$) light emission from $\text{SrAl}_2\text{O}_4 : \text{Eu,Dy}$ as proposed by Clabau et al.²⁹ occurs due to detrapping of trapped electrons directly to the 5d levels of Eu^{3+} (due to the trapping processes, Eu^{2+} is oxidized to Eu^{3+}). The 450 nm emission (at lower temperatures) is observed due to a charge transfer from the level $4f^7$ configuration of Eu^{2+} (residual Eu^{3+} is reduced to Eu^{2+}) to the valence band and is associated with the hole detrapping mechanism. Thus emissions from the phosphors are basically a detrapping process that occurs due to thermal energy available at ambient temperature. Thermal energy (kT_{RT}) required for detrapping can be written as $(kT_{RT}-E)$, where E would be energy dissipated to the polymer matrix. This can be shown in the schematic illustration, as shown in Scheme 3.



Scheme 3 Tentative mechanism for the emission spectra.

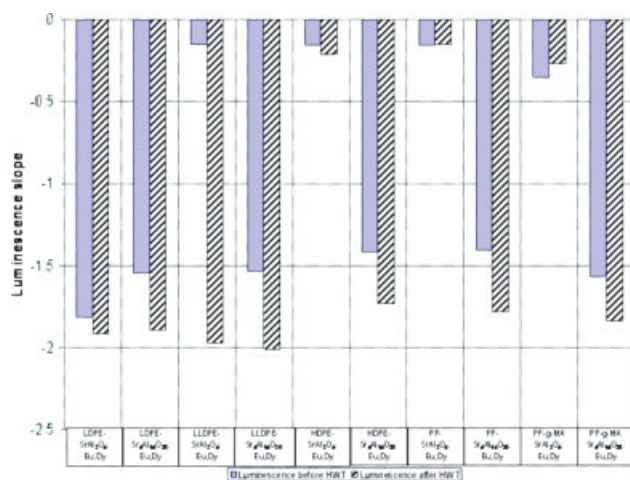


Figure 4 Decay curve slopes of polymer-phosphor composites. [Color figure can be viewed in the online issue, which is available at www.interscience.wiley.com.]

This would probably allow only part of the thermal energy available for the detrapping process resulting in an overall delay of the phosphorescence mechanism observed as poor intensity of the luminescence. The other contributing factors for the decrease in luminescent intensities are the attenuation of photons through the polymer matrix and the low concentration of the phosphor in the composite.

Hamburg wheel tests

Hamburg tests were conducted to evaluate the durability of the polymers against simulated wheel loads and the effect of these wheel loads on the luminosity of the polymers. The data in Figure 4 compare the slope values of the decay curves (luminosity versus time) of the different polymer-phosphor composites. A steep slope (large value) indicates quicker luminosity decay rates. The bar graph suggests that the duration of luminosity for polymer-Sr₄Al₁₄O₂₅:Eu,Dy composites were shorter than those of polymer-SrAl₂O₄:Eu,Dy composites especially for the HDPE, PP, PP-g-MA. In the case of the PP-SrAl₂O₄:Eu,Dy and the PP-g-MA-SrAl₂O₄:Eu,Dy composites, the duration of luminescence remained either similar or increased after the HWT test. The mechanical stimulus such as grinding and friction on the surface of the sample allows more of the phosphors embedded in the polymer to become freely available for the absorbance of UV light. However, the wheel load of 705 N might affect the crystal structure of some of the phosphor particles at the level of a unit cell, thereby affecting the phosphorescence process resulting in a shorter duration of luminosity after HWT test.

CONCLUSIONS

Polymer and strontium aluminate phosphor composites were prepared using a melt mixing and extrusion technique. The morphologies of the prepared polymer-phosphor composites show various leaf patterns, which differ slightly depending upon the densities and viscosities of the polymers. The luminescent behavior of the composites primarily gets affected by the opacity and resistance of a matrix for the UV radiations besides refractive indices of the medium. Thermal energy available at an ambient temperature for the detrapping would partially be dissipated to matrices affecting the detrapping process and resulting in low to poor intensities. The wavelengths of the emissions were, however, not influenced. The luminescent property of the phosphor composites is sustained even after performing the HWT. However, the duration of luminosity is reduced after HWT test for various polymer-phosphor composites. PP-SrAl₂O₄:Eu,Dy and PP-g-MA-SrAl₂O₄:Eu,Dy composites show the longest duration for the decay.

The authors thank Prof P.W.J. van Wyk from the Centre of Confocal and Electron Microscopy for SEM analysis.

References

- Wang, H.; Lu, X.; Zhao, Y.; Wang, C. *Mater Lett* 2006, 60, 2480.
- Zhang, P.; Xu, M.; Zheng, Z.; Liu, L. *J Sol-Gel Sci Technol* 2007, 43, 59.
- Smets, B.; Rutten, J.; Hoeks, G. *J Electrochem Soc* 1989, 136, 2119.
- Nakazawa, E.; Murazaki, Y.; Saito, S. *J Appl Phys* 2006, 100, 1131131.
- Matsuzawa, T.; Aoki, Y.; Takeuchi, N.; Murayama, Y. *J Electrochem Soc* 1998, 143, 2670.
- Lu, Y.; Li, Y.; Xiong, Y.; Wang, D.; Yin, Q. *Microelectron J* 2004, 35, 379.
- Murayama, Y.; Takeuchi, N.; Aoki, Y.; Matsuzawa, T. *U.S. Pat.* 5,424,006 (1995).
- Katsumata, T.; Nabae, T.; Sasajima, K.; Kumuro, S.; Morikawa, T. *J Electrochem Soc* 1997, 144, L243.
- Yamamoto, H.; Matsuzawa, T. *J Lumin* 1997, 72-74, 287.
- Groppi, G.; Cristiani, C.; Forzatti, P. *J Mater Sci* 1994, 29, 3441.
- Jia, W. Y.; Yuan, H. B.; Yen, W. M. *J Lumin* 1998, 76, 424.
- Toh, K.; Nagata, S.; Tsuchiya, B.; Shikama, T. *Nucl Instrum Methods Phys Res Sect A* 2006, 249, 209.
- Lin, Y.; Tang, Z.; Zhang, Z. *Mater Lett* 2001, 51, 14.
- Peng, T.; HuaJun, L.; Yang, H.; Yan, C. *Mater Chem Phys* 2004, 85, 68.
- Molina, C.; Dahmouche, K.; Santilli, C. V.; Craievich, A. F.; Ribeiro, S. J. L. *Chem Mater* 2001, 13, 2818.
- Sanchez, C.; Ribot, F. *New J Chem* 1994, 18, 1007.
- Feng, S.; Xu, R. *Acc Chem Res* 2001, 34, 239.
- Ferey, G. *Chem Mater* 2001, 13, 3084.
- Rao, C. N. R.; Natarajan, S. *Vaidhyanathan, T. Angew Chem Int Ed Engl* 2004, 43, 1466.
- Wang, D.; Zhang, J.; Lin, Q.; Fu, L.; Zhang, H.; Yang, B. *J Mater Chem* 2003, 13, 2279.

21. Peng, L.; Luo, Y.; Dan, Y.; Zhang, L.; Zhang, Q.; Xia, S.; Zhang, X. *Colloid Polym Sci* 2006, 285, 153.
22. Abdullah, M.; Waris, K. A.; Sutrisno, W.; Nurhasanah, I.; Vioktalamo, A. S. *Powder Technol* 2008, 183, 297.
23. Wang, L.; Sasaki, T.; Ebina, Y.; Kurashima, K.; Watanbe, M. *Chem Mater* 2002, 14, 4827.
24. Susa, A. S.; Caruso, F.; Rogach, A. L.; Sukhorukov, G. B.; Kornowski, A.; Mohwald, H.; Giersig, M.; Eychmuller, A.; Weller, H. *Colloids Surf A* 2000, 163, 39.
25. Dennis, H. R.; Hunter, D.; Chang, D.; Kim, S.; Paul, D. R. *Polymer* 2001, 42, 9513.
26. Harnath, D.; Shanker, V.; Chander, H.; Sharma, P. *J Phys D: Appl Phys* 2003, 36, 2244.
27. Sun, J. Y.; Shi, C. S.; Li, Y. M. *Chin Sci Bull* 1989, 34, 703.
28. Bhat, S. V.; Govindraj, A.; Rao, C. N. R. *Chem Phys Lett* 2006, 422, 323.
29. Clabau, F.; Rocquefelte, X.; Jobic, S.; Deniard, P.; Whangbo, M.-H.; Garcia, A.; Le Mercier, T. *Chem Mater* 2005, 17, 3904.